CHEMICAL ENGINEERING TRANSACTIONS
VOL. 96, 2022
A publication of AIDIC
The Italian Association of Chemical Engineering
Online at www.cetjournal.it
Guest Editors: David Bogle, Flavio Manenti, Piero Salatino

ISBN 978-88-95608-95-2; **ISSN** 2283-9216
DOI: 10.3303/CET2296008

Magnesium Hydroxide Nanoparticles Production from Natural Bitterns

Giuseppe Battaglia, Maria Alda Domina, Salvatore Romano, Alessandro Tamburini, Andrea Cipollina*, Giorgio Micale

Dipartimento di Ingegneria, Università degli Studi di Palermo, Viale delle Scienze Ed. 6, 90128 Palermo, Italy
andrea.cipollina@unipa.it

Magnesium hydroxide nanoparticles are widely employed in numerous industrial applications. Several preparation methods have been proposed using mainly synthetic Mg^{2+} containing solutions. In the present work, the possibility of producing $Mg(OH)_2$ nanoparticles from real bitterns, the by-product of sea salt production, is investigated. Bitterns are highly concentrated Mg^{2+} containing solutions whose exploitation can turn a waste into valuable products embracing the circular economy idea. Two bitterns collected from Galia and Margi saltworks of the district of Trapani (Italy) were studied. Galia and Margi bitterns had a 1 M and 2.5 M Mg^{2+} concentration, respectively. A 2 mm diameter circular-cross sectional T-mixer was adopted to ensure fast reactant mixing. NaOH solutions were employed as precipitant agents. $Mg(OH)_2$ nanoparticles characterized by cationic and mass purity higher than 99 % and 90 %, respectively, were successfully produced when treating Galia bitterns, while the excessive Margi Mg^{2+} concentration yielded stronger micrometer $Mg(OH)_2$ agglomerates.

1. Introduction

In the last decades, nanoparticles have attracted much interest for their peculiar characteristics, e.g. superconductivity, thermal stability, non-linear optics, etc. (Qiu et al., 2003). Polymers embodying nanoparticles have also been widely investigated for their superior features with respect to those exhibited by materials embodying micrometer particles (Qiu et al., 2003). In this context, magnesium hydroxide, $Mg(OH)_2$, nanoparticles have been extensively employed in numerous applications (Balducci et al., 2017). Pilarska et al (Pilarska et al., 2013) studied the synthesis of magnesium hydroxide nanoparticles as the precursor for the production of magnesium oxide (MgO) catalysts. $Mg(OH)_2$ was precipitated from magnesium sulfate and sodium hydroxide (NaOH) by precipitation. Non-ionic poly(ethylene glycols) compounds with different molecular weights were added as surface modifiers. The authors successfully produced $Mg(OH)_2$ nanoplates that, after calcination, formed MgO particles with a high surface area. Pan et al. (Pan et al., 2013) studied the antibacterial activity of $Mg(OH)_2$ nanoparticles on Escherichia coli. $Mg(OH)_2$ nanoparticles were synthesized using NaOH and different Mg solutions. The best antibacterial action was exhibited by $Mg(OH)_2$ particles precipitated from magnesium chloride ($MgCl_2$) solutions. Ren et al. (Ren et al., 2016) studied the production of nano $Mg(OH)_2$ particles for flame retardant applications. The authors synthesized nano $Mg(OH)_2$ particles employing a reactor able to achieve very short mixing times. $Mg(OH)_2$ nanoparticles were then modified by adopting a hydrothermal treatment. It was found that high-grade $Mg(OH)_2$ flame retardant particles can be obtained using NaOH concentrations ≥ 2.4 M, hydrothermal time ≥ 3 h, hydrothermal temperature ≥ 170 °C and solid content ≤ 6.0 wt%. Park et al. (Park et al., 2018) investigated the effect of the addition of $Mg(OH)_2$ nanoparticles into porous polymer scaffolds to neutralize the release of acid products during scaffold degradation. The $Mg(OH)_2$ neutralization action was found to be effective against the acid release. Battaglia et al. (Battaglia et al., 2022) assessed the crucial role of reactants mixing in the $Mg(OH)_2$ precipitation process. The authors employed two circular cross-sectional T-mixers with internal diameters respectively of 3 and 2 mm to tune the mixing degree between 1 M $MgCl_2$ and 2 M NaOH synthetic solutions. T-mixers were employed thanks to the short mixing times achieved in such systems (Romano et al., 2021). $Mg(OH)_2$ nanoflakes were obtained when the mixing time between reagents was shorter than 2 ms.

Paper Received: 14 January 2022; Revised: 2 July 2022; Accepted: 2 August 2022
Please cite this article as: Battaglia G., Domina M.A., Romano S., Tamburini A., Cipollina A., Micale G., 2022, Magnesium Hydroxide Nanoparticles Production from Natural Bitterns, Chemical Engineering Transactions, 96, 43-48 DOI:10.3303/CET2296008

The authors also highlighted the need for an anti-agglomerant treatment, i.e. the use of dispersant and sonication, to assess the actual assemblage state of produced $Mg(OH)_2$ particles.
In the last years, attention has been placed on the development of green processes for the production of nanoparticles (Reverberi et al., 2017). Up to now, however, the majority of commercial $Mg(OH)_2$ products are synthesized by employing Mg containing minerals (Luong et al., 2018) and seawater using dolomitic lime (Jakić et al., 2016). These processes require high energy and cause mineral depletion. Luong et al. (Luong et al., 2018) also analysed the carbon footprint of $Mg(OH)_2$ production from bischofite brines and serpentinite ores. 1.6E3.3 kg CO_2eq/kg $Mg(OH)_2$ and 2.6E5.2 kg CO_2eq/kg $Mg(OH)_2$ were calculated for bischofite brine and serpentinite processes, respectively. $Mg(OH)_2$ manufacturing through clean and sustainable processes represents, therefore, a crucial opportunity to reduce the environmental impact of $Mg(OH)_2$ production. In this context, the European Horizon 2020 SEArcularMINE project aims at developing a novel sustainable integrated process for the valorization of exhausted bitterns, the by-product of sea salt production, targeting, among the others, Mg recovery in the form of $Mg(OH)_2$.
The present work, performed within the SEArcularMINE activities, addresses the feasibility of $Mg(OH)_2$ nanoparticles synthesis from two real bitterns collected from Galia (1 M Mg^{2+}) and Margi (2.5 M Mg^{2+}) saltworks located in the district of Trapani (Sicily, Italy). A 2-mm diameter circular cross-sectional T-mixer has been adopted to achieve short mixing times and a fast mixing of the reactants, thus promoting the production of nanoparticles, as extensively discussed in the literature (Battaglia et al., 2022). NaOH was employed as precipitating agent, while, for the first time, bitterns were adopted as feed stream containing Mg^{2+}. Particle size distributions were obtained by static light scattering technique with and without an anti-agglomerant treatment. In addition, particles' purity was assessed by ionic chromatography and thermogravimetric analyses.

2. Material and Methods

Magnesium hydroxide precipitation from real bitterns was carried out employing a 2 mm circular cross-sectional T-mixer drilled into a polymethyl methacrylate (PMMA) block. The T-mixer was made of 2 cm long horizontal pipes merging into a 4 cm long vertical channel, also called mixing channel. An insight of the T-mixer is illustrated in the left part of Figure 1. Reacting solutions were withdrawn from two containing flasks and fed to the T-mixer by means of two gear pumps (Fluid-o-Tech® FG200/FG300 series) controlled by a dedicated LabVIEW code.

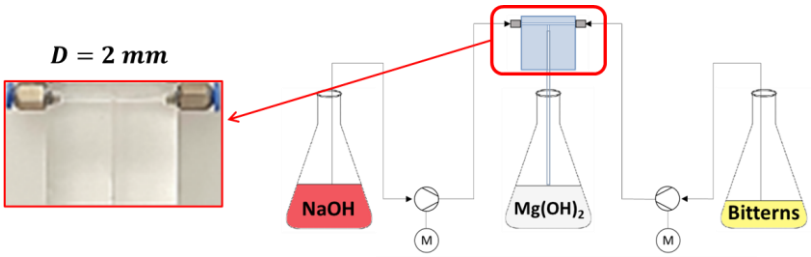

Figure 1 Schematic drawing of the experimental set-up. On the left, an insight of the employed 2 mm circular cross-sectional T-mixer.

The $Mg(OH)_2$ precipitation occurs through the reaction between hydroxyl and magnesium ions forming sparingly soluble $Mg(OH)_2$ powders, as reported in Eq. (1):

$$Mg^{2+}(aq) + 2\,OH^{-}(aq) + 2\,Na^{-}(aq) \rightarrow Mg(OH)_2(s) + 2\,Na^{-}(aq) \quad (1)$$

In the present work, $Mg(OH)_2$ powders were synthesized using Margi and Galia bitterns treated with synthetic NaOH solutions. NaOH solutions were made by dissolving NaOH pellets (Honeywell|Fluka™, purity > 98 %) in deionized water and their concentrations verified by titration.
Bitterns' Mg^{2+} composition was assessed through Ion Chromatography (IC, Metrohm 882 Compact IC plus) analysis. NaOH solutions and bittern Mg^{2+} concentrations are reported in Table 1.

2.1 Experimental tests and procedure

$Mg(OH)_2$ particles were synthesized by performing stoichiometric and 20% OH^- excess precipitation experiments. The same 2 mm diameter T-mixer employed by Battaglia et al. (Battaglia et al., 2022) was used. Battaglia et al. obtained $Mg(OH)_2$ nanoparticles from 1 M $MgCl_2$ and 2 M NaOH synthetic solutions when the mean fluid flow velocity in the mixing channel was 12 m/s (a total flow rate of ~2320 mL/min). In the present

work, due to the high Mg^{2+} content in the Margi bitterns, i.e. ~2.5 M, at least a 5 M NaOH solution would be needed if the same solution flow rate had been used. To avoid handling hazardous solutions, the NaOH flow rate was doubled with respect to that of bitterns' one, targeting the same total flow rate in the mixing channel employed by Battaglia et al. (Battaglia et al., 2022), i.e. ~2320 mL/min. Table 1 presents details of the experimental tests. Each experiment was conducted twice for reproducibility purposes.

Table 1 Operating conditions of experimental tests.

Tests	*Bittern solution*	*OH^-/ Mg^{2+}*	*Bittern flowrate (mL/min)*	*NaOH/Bittern flowrate ratio*	*Mg^{2+} concentration (M)*	*NaOH concentration (M)*
M_S	*Margi*	*Stoichiometric*	*780±20*	*2*	*2.48±0.05*	*2.50±0.05*
M_E	*Margi*	*20% excess of OH-*	*780±20*	*2*	*2.48±0.05*	*3.00± 0.06*
G_S	*Galia*	*Stoichiometric*	*780±20*	*2*	*0.96±0.18*	*1.00± 0.02*
G_E	*Galia*	*20% excess of OH-*	*780±20*	*2*	*0.96±0.18*	*1.20± 0.02*

After precipitation, $Mg(OH)_2$ suspensions were collected in a receiving flask. Part of the suspension was immediately analysed by using the static light scattering Malvern Mastersizer2000 granulometer equipped with the Hydro 2000 MU dispersant unit. All measurements were conducted by setting the Hydro 2000 MU stirrer velocity at 2000 rpm. Volume particle size distributions (V-PSDs) were obtained with and without sonication and the addition of the poly(acrylic acid, sodium salt), (PAA, MW 1200, Sigma-Aldrich, Inc.) as a dispersant. V-PSD measurements were performed as follows: (i) 30 PAA drops were added into the Hydro 2000 MU beaker filled with 700 mL deionized water and the background was acquired; (ii) $Mg(OH)_2$ suspension was added until the light obscuration was ~24 %; (3) 5 V-PSDs measurements were conducted; (4) 5 mins of sonication were applied through the Hydro 2000 MU integrated ultrasound probe at 20 kHz; (5) 5 further V-PSDs measurements were collected. Experiments were conducted twice for reproducibility purposes. Average V-PSDs between repeated tests (10 curves in total) are shown in Figure 2 along with error bars considering both tests repeatability and multiple V-PSDs measurements uncertainty. The remaining $Mg(OH)_2$ suspension was filtrated using a Buchner funnel and 1.8 µm glass fiber filters (GE Healthcare Life Science Whatman™). $Mg(OH)_2$ cake was then washed with a deionized water volume equal to that of the filtrated suspension. The cake was then dried at 105 °C in an oven for 24 h. (i) ~100 mg $Mg(OH)_2$ powder was dissolved in 1 M hydrochloric acid (HCl, Honeywell|FlukaTM) for cation content assessment through IC; (ii) ~80-200 mg was used for mass purity assessment via Thermogravimetric Analysis (TGA, STA 449 F1 Jupiter analyzer, NETZSCH); (iii) few grams were also employed for morphology observation using the Scanning Electron Microscopy (SEM FEI Quanta 200 FEG) equipment. TGA analyses were conducted with a heating rate of 10 °C/min from 30 °C to 1000 °C, under a constant nitrogen flow of 20 mL/min.

2.2 Cationic and mass purity

$Mg(OH)_2$ cationic purity was determined as the Mg^{2+} ions concentration contained in dissolved powders over the total cation species concentration detected by the IC technique:

$$Cationic\ purity = \frac{C_{Mg2+}}{\sum_{i=1}^{N} C_i} * 100 \quad (2)$$

where C_i is the concentration of the i-th cation species and N is the total number of detected cations.
$Mg(OH)_2$ mass purity was calculated considering the $Mg(OH)_2$ mass over the dry sample mass:

$$Mass\ purity\ \% = \frac{m_{Mg(OH)2}^{\Delta T=320-480°C}}{m_{sample}^{Total} - m_{H2O}^{\Delta T=30-200°C}} * 100 \quad (3)$$

In Eq. (3), $Mg(OH)_2$ mass, $m_{Mg(OH)_2}^{\Delta T=320-480°C}$, was obtained by considering the water mass loss detected between 320 °C and 480 °C in the TG analysis. The dry sample mass was calculated by subtracting the sample humidity, $m_{H2O}^{\Delta T=30-200°C}$, to the initial total sample mass, m_{sample}^{Total}. The humidity content was assessed as the water loss measured between 30 °C and 200 °C.

3. Results

$Mg(OH)_2$ particles produced from natural bitterns were characterized in terms of particles sizes, morphology and purity. Particles size distributions and SEM images are discussed in Section 3.1. Cationic and mass purity values are reported in Section 3.2.

3.1 Particle granulometry and shapes

Volume particle size distributions of $Mg(OH)_2$ particles precipitated from Margi and Galia bitterns under stoichiometric and 20 % OH^- hydroxyl ions conditions are presented in Figure 2. V-PSDs were obtained with (Figure 2.b and 2.d) and without (Figure 2.a and 2.c) sonication. The anti-agglomerant PAA agent was used in all analysis.

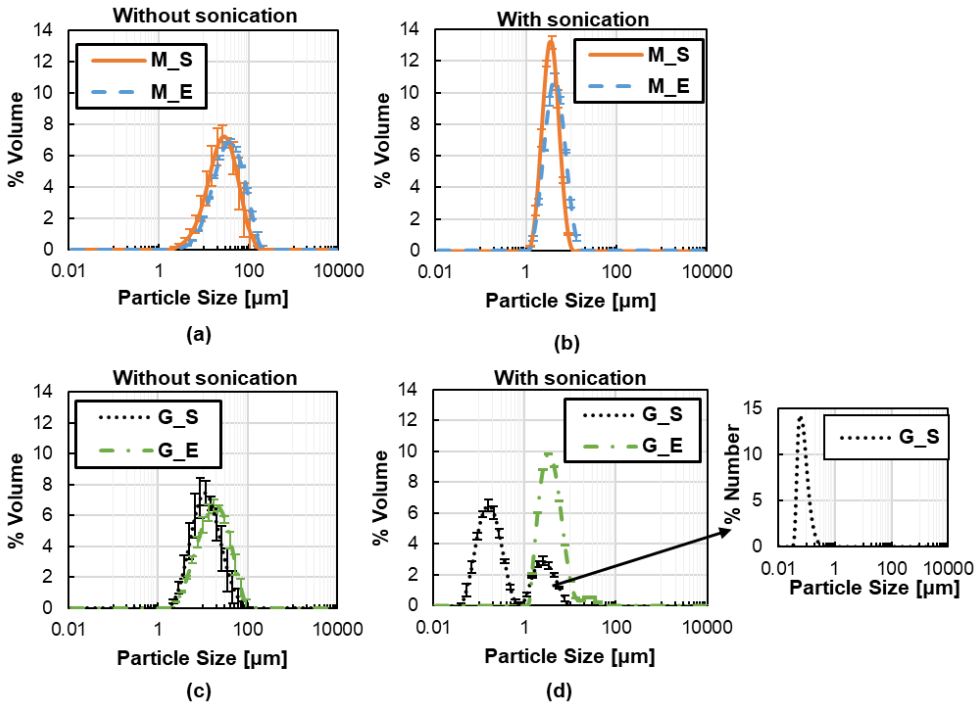

Figure 2 Volume particle size distributions of $Mg(OH)_2$ particles precipitated from Margi and Galia bitterns under stoichiometric (M_S and G_S) and 20 % OH^- excess conditions (M_E and G_E): (a) and (c) without sonication; (b) and (d) with sonication treatment. The anti-agglomerant PAA agent was used in all analysis. For the G_S case also its corresponding Number size distribution is reported.

Similar V-PSDs are observed in the absence of sonication regardless of the employed bittern or precipitation condition, see Figure 2.a and 2.c. Specifically, particles range between 1 and 100 µm. Particle dimensions decrease after sonication. Narrow V-PSDs from 1 to 10 µm are observed both for M_S and M_E samples, as shown in Figure 2.b. Conversely, a considerable particle size variation is noticed in the G_S sample. Specifically, a bi-modal distribution is observed. Particles range between 0.06-0.6 µm and 1-10 µm. Large particles can be either attributed to impurities or co-precipitated compounds due to the bittern real nature. In this case, also the number particle size distribution (NSD) is reported. NSD provides information regarding the number percentages of particles with a certain dimension. In the NSD, particles range between 0.02 and 0.2 µm, thus demonstrating the main presence of nanoparticles in the suspension. Such a result is not attained for the G_E sample where particles range between 1-10 µm. In the absence of sonication, weak agglomerates, i.e. particles kept together by electrostatic forces, are mainly measured due to the un-stable nature of $Mg(OH)_2$ particles characterized by low zeta-potential values varying from ~ +23 mV at pH 10 to ~ -23 mV at pH 13 (Battaglia et al., 2022), thus similar V-PSDs are observed in Figure 2.a and 2.c. On the other hand, the application of the PAA dispersant agent and sonication allows the measurement of either strong agglomerates or aggregates. Strong agglomerates are aggregates kept together by strong bridges that can be still broken down after the application of a strong external force (a long duration of ultrasounds, e.g. >10 mins). Aggregates are primary particles linked by chemical bonds that cannot be broken down by the application of sonication. Therefore, Figure 2.a and 2.c

refer to $Mg(OH)_2$ agglomerates size distributions, while Figure 2.b and 2.d report the size distributions of strong agglomerates for M_S, M_E and G_E samples and aggregates for the G_S case. Considering the M_S and G_S cases, only the G_S sample presents nanoparticles. This is mainly due to the very high Mg^{2+} concentration in the Margi bittern which requires an even shorter mixing time than that achieved in the employed T-mixer. Conversely, Galia bittern has a similar Mg^{2+} concentration as that employed by Battaglia et al. (Battaglia et al., 2022), that can be successfully homogenized by the employed T-mixer and operating parameters. Regarding V-PSDs obtained for M_E and G_E samples, it can be expected that the suspension pH would be ~12 during all the $Mg(OH)_2$ precipitation process due to the employed OH^- excess. At such pH value, the $Mg(OH)_2$ zeta-potential reaches its iso-electric point (null zeta-potential condition, the highest un-stable condition for the particles) increasing particle agglomeration tendency that, in turn, enhances particle sticking probability eventually favoring the formation of bridges between aggregates. A SEM image of $Mg(OH)_2$ particles obtained for case G_S is reported in Figure 3. For the sake of brevity, no other SEM images are reported as very similar results are obtained among the other experimental tests.

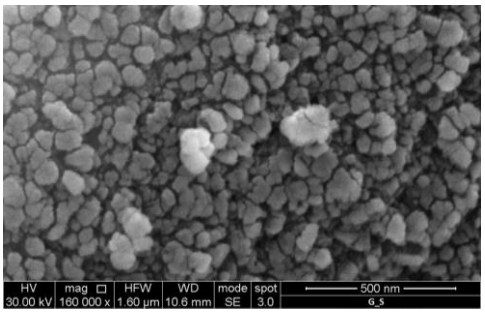

Figure 3 A SEM image of $Mg(OH)_2$ nanoparticles obtained for the G_S sample.

Nanoflakes and globular MH particles can be observed in Figure 3 with dimensions between few nanometers to 0.200 µm, in accordance with the G_S NSD shown in Figure 2.d.

3.2 Cationic and Mass Purity

In Section 3.1, V-PSDs of $Mg(OH)_2$ particles precipitated from Galia bitterns under stoichiometric conditions demonstrated the possibility of producing nanoparticles from exhausted saltworks bitterns. Due to the nature of the initial Mg^{2+} containing solutions, particles' cationic and mass purity were investigated. Table 2 reports cation concentrations measured by IC in dissolved $Mg(OH)_2$ powders along with calculated cationic purity values, Eq.(2). Furthermore, humidity, $Mg(OH)_2$ mass percentage measured by TG analysis and dry based mass purity calculations, Eq.(3), are also reported.

Table 2 Cationic and mass purity of $Mg(OH)_2$ samples precipitated from Margi and Galia bitterns. Cation concentrations in dissolved $Mg(OH)_2$ powders, measured by IC, humidity and $Mg(OH)_2$ mass percentage, measured by TG analysis, are also reported.

Tests	Ca^{2+} (mg/g, IC)	Mg^{2+} (mg/g, IC)	Na^+ (mg/g, IC)	Cationic Purity (IC) %	Humidity (TG) %	$Mg(OH)_2$ mass (TG) %	Dry Mass Purity (TG) %
M_S	LOQ	376 ± 1	1.8 ± 0.5	>99	2.3	88	90
M_E	LOQ	375 ± 2	3.5 ± 0.1	>99	3.6	89	93
G_S	LOQ	371 ± 3	2.5 ± 1.1	>99	3.3	91	94
G_E	LOQ	376 ± 1	LOQ	>99	3.9	93	97

Cationic purity is always higher than 99 % in all samples, i.e. Mg^{2+} ions are the main cations present in the synthesized $Mg(OH)_2$ powders. Mass purity values, however, are higher than 90 % but do not reach 100 % values. The main expected contaminants in the particles are magnesium carbonate ($MgCO_3$) and Boron compounds. $MgCO_3$ is likely to be formed by carbonation due to the CO_2 presence in the precipitation water system (Verri, 1997). Boron compound traces have been reported in the literature since Boron is adsorbed into $Mg(OH)_2$ surface (Shand, 2006).

4. Conclusions

The production of $Mg(OH)_2$ nanoparticles from real bitterns was investigated. Volume Particle size distributions (V-PSDs) of $Mg(OH)_2$ particles precipitated under stoichiometric and 20 % OH^- conditions were measured by static light scattering technique with and without the use of an anti-agglomerant treatment. Without the anti-agglomerant treatment, similar V-PSDs ranging from 1 μm to 100 μm, characteristics of $Mg(OH)_2$ weak agglomerates, were observed regardless of bitterns and precipitation conditions. Conversely, narrow V-PSDs in the range from 1 μm to 10 μm, associated with strong $Mg(OH)_2$ agglomerates, were measured after particle treatment. $Mg(OH)_2$ nanoparticles ranging from 0.02 μm to 0.2 μm were produced only using Galia bitterns under stoichiometric conditions. This was attributed to the lower Mg^{2+} concentration in Galia bitterns with respect to that of Margi ones and the lower pH value during the precipitation process with respect to OH^- excess cases. $Mg(OH)_2$ particles cationic and mass purity were also investigated. Cationic purity was always higher than 99 %, while mass purity ranged from 90 % to 95 %. Overall, high purity $Mg(OH)_2$ nanoparticles were successfully produced from real exhausted Galia bitterns demonstrating the possibility of valorizing a waste to produce valuable products in the concept of the circular economy. A scale up of the proposed approach will be carried out in the second phase of the SEArcularMINE project aiming at exploiting the bitterns potential as Mg source. In the best scenario, this has been estimated to satisfy more than 30 % of the worldwide $Mg(OH)_2$ demand.

Acknowledgments

This project has received funding from the European Union's Horizon 2020 research and innovation programme under Grant Agreement No. 869467 (SEArcularMINE). This output reflects only the author's view. The European Health and Digital Executive Agency (HaDEA) and the European Commission cannot be held responsible for any use that may be made of the information contained therein.

References

Balducci, G., Bravo Diaz, L., Gregory, D. H., 2017, Recent progress in the synthesis of nanostructured magnesium hydroxide, CrystEngComm, 19(41), 6067–6084.

Battaglia, G., Romano, S., Raponi, A., Marchisio, D., Ciofalo, M., Tamburini, A., Cipollina, A., Micale, G., 2022, Analysis of particles size distributions in Mg(OH)2 precipitation from highly concentrated MgCl2 solutions, Powder Technology, 398, 117106.

Jakić, J., Labor, M., Martinac, V., 2016, Characterization of dolomitic lime as the base reagent for precipitation of Mg(OH)2 from seawater, Chemical and Biochemical Engineering Quarterly, 30(3), 373–379.

Luong, V. T., Amal, R., Scott, J. A., Ehrenberger, S., Tran, T., 2018, A comparison of carbon footprints of magnesium oxide and magnesium hydroxide produced from conventional processes, Journal of Cleaner Production, 202, 1035–1044.

Pan, X., Wang, Y., Chen, Z., Pan, D., Cheng, Y., Liu, Z., Lin, Z., Guan, X., 2013, Investigation of antibacterial activity and related mechanism of a series of nano-Mg(OH)2, ACS Applied Materials and Interfaces, 5(3), 1137–1142.

Park, K. S., Kim, B. J., Lih, E., Park, W., Lee, S. H., Joung, Y. K., Han, D. K., 2018, Versatile effects of magnesium hydroxide nanoparticles in PLGA scaffold–mediated chondrogenesis, Acta Biomaterialia, 73, 204–216.

Pilarska, A., Wysokowski, M., Markiewicz, E., Jesionowski, T., 2013, Synthesis of magnesium hydroxide and its calcinates by a precipitation method with the use of magnesium sulfate and poly(ethylene glycols, Powder Technology, 235, 148–157.

Qiu, L., Xie, R., Ding, P., Qu, B., 2003, Preparation and characterization of Mg(OH)2 nanoparticles and flame-retardant property of its nanocomposites with EVA, Composite Structures, 62(3–4), 391–395.

Ren, M., Yang, M., Li, S., Chen, G., Yuan, Q., 2016, High throughput preparation of magnesium hydroxide flame retardant: Via microreaction technology, RSC Advances, 6(95), 92670–92681.

Reverberi, A. P., Vocciante, M., Lunghi, E., Pietrelli, L., Fabiano, B., 2017, New trends in the synthesis of nanoparticles by green methods, Chemical Engineering Transactions, 61, 667–672.

Romano, S., Battaglia, G., Bonafede, S., Marchisio, D., Ciofalo, M., Tamburini, A., Cipollina, A., Micale, G., 2021, Experimental Assessment of the Mixing Quality in a Circular Cross-sectional T-shaped Mixer for the Precipitation of Sparingly Soluble Compounds, Chemical Engineering Transactions, 86, 1165–1170.

Shand, M. A., 2006, The chemistry and technology of magnesia. Wiley-Interscience.

Verri, G., 1997, Process for the purification of magnesium hydroxide. Patents.google.com/patent/US5626825A/en